

# Droplet break-up investigations in scaled high-pressure homogenizers with orifice plates

Benedikt Mutsch<sup>1\*</sup>, Christian J. Kähler<sup>1</sup>

<sup>1</sup> Universität der Bundeswehr München, Institute of Fluid Mechanics and Aerodynamics, Neubiberg, Germany

\* benedikt.mutsch@unibw.de

## Abstract

The drop break-up in a scaled test rig for high-pressure homogenization of emulsion with orifices as fragmentation unit was investigated using optical measurement techniques. 2D2C PIV measurements were performed to characterize the mean and unsteady flow field in the test rig. The visualization of droplets is done by shadowgraphy. In order to visualize the oil droplets in the continuous aqueous phase with high contrast a novel shadowgraphy methods was developed and implemented. According to our results the droplet break-up does not occur due to the elongation in the laminar flow region in the orifice inlet. This causes only a deformation of the droplet towards a filament, which occurs especially with low-viscosity droplets. Instead, the drop break-up occurs in the turbulent shear layer of the free jet behind the orifice and is primarily caused by turbulent vortices. The typically obtained drop size distribution of high pressure homogenization results from the uneven stress distributions of the drops based on the turbulence characteristics of the jet and trajectory of the drop.

## 1 Introduction

High pressure homogenizers are often used in the chemical, pharmaceutical and food industries for the production of emulsions, these are mixtures of two or more insoluble fluids. In conventional high-pressure homogenizers, it is difficult to investigate the process of droplet break-up and other ongoing processes using optical measuring methods, as the systems are under very high pressure and therefore made out of steel. In addition, the geometric dimensions of the fragmentation units are very small. Furthermore the high pressure and the narrow channel cross-sections inevitably result in a very fast flow, making optical investigations very difficult and time-resolved measurements almost impossible (Kähler et al. (2016)). To make systematic investigations on the droplet break-up possible, a scaled test facility was developed that is geometrically similar to the original facility. In order to be able to transfer the results of the experiment to the original scale and process, the material and process parameters were also scaled so that a geometrically and physically similar process can be analyzed and the results can be compared (Walzel (2015)). A particular advantage of scaling the system is that the differential pressure and thus the flow velocity decrease for the same Reynolds number, thus making investigations much simpler (Walzel (2015)). In this paper the results of the measurements in the scaled test facility are presented. A detailed description of the test facility and the measures taken for scaling can be found in Mutsch and Kähler (2017).

## 2 Theoretical background

Drop break-up has been studied for many decades, with the beginnings going back to Taylor 1934 (Taylor (1934)). In this study, as well as in most subsequent ones, the laminar droplet break-up was investigated. This is still a frequently investigated case in recent investigations, even though turbulent conditions prevail mainly in today's emulsifying applications. The aim of investigating laminar drop break-up is to determine the limits of break-up, i.e. the minimum stresses at which drop break-up just occurs. In laminar flow conditions, the dimensionless Capillary number ( $Ca$ ) is used as a measure of the drop loading (see Eq. 1). The capillary number is the ratio of the external laminar stress caused by the flow and transferred from the

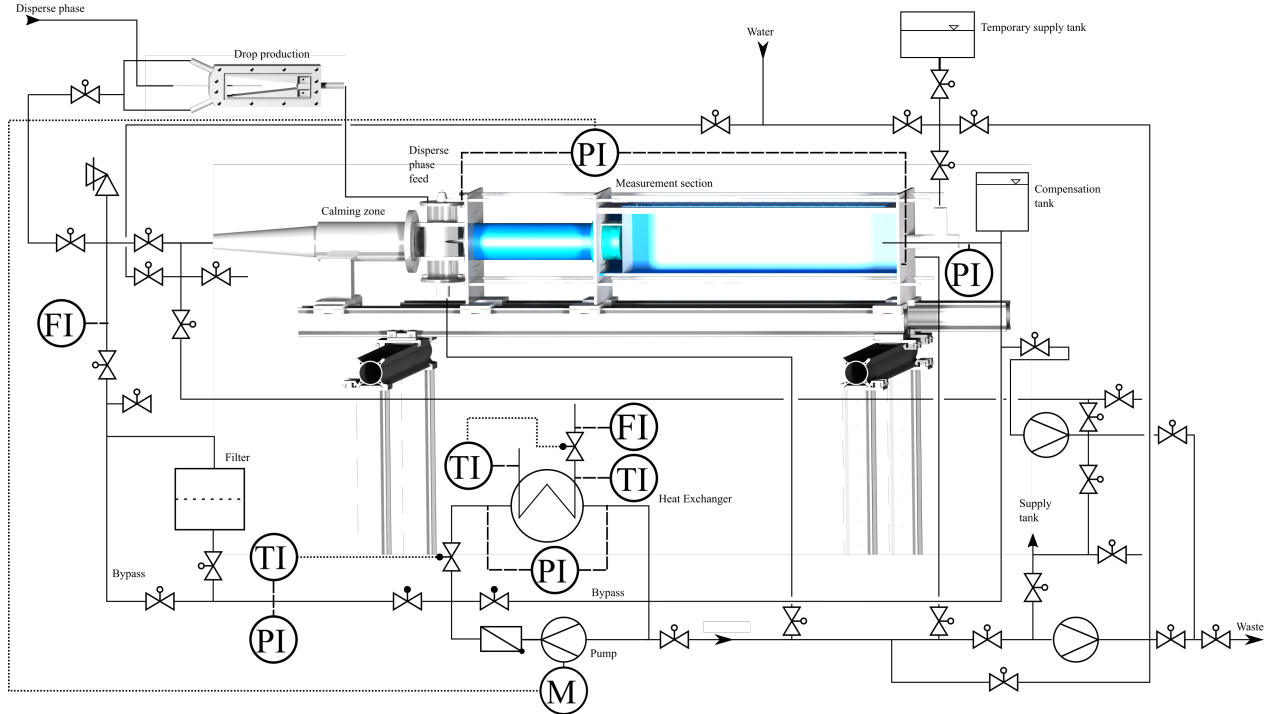


Figure 1: Process Flow Diagramm of the test rig.

continuous phase to the droplets of the disperse phase, and the restoring internal forces of the droplet, which are mainly determined by the surface tension ( $\sigma$ ). The external forces are determined from the dynamic viscosity of the continuous phase ( $\eta_c$ ), the shear rate ( $\dot{\gamma}$ ) and the droplet diameter ( $D$ ) (Mighri and Huneault (2006)).

$$Ca = \frac{\eta_c \cdot \dot{\gamma} \cdot D}{\sigma} \quad (1)$$

The result of these investigations is that there is a critical capillary number for fluid systems with viscosity ratios ( $\eta^*$ , see Eq. 2) less than about 4. Systems with higher viscosity ratios do not break in laminar flow according to Walstra (1993).

$$\eta^* = \frac{\eta_d}{\eta_c} \quad (2)$$

In turbulent flows, different areas of drop break-up are distinguished. The differentiation is based on the size ratio between the energy-carrying vortices and the droplet size. Turbulence with vortices larger than the droplet size is referred to as turbulent viscous regime (TV). The drop decay in the area where the vortices are smaller than the drops is called the turbulent inert regime (TI). In the TV regime the droplets are deformed and stressed by viscous forces caused by the large vortices, whereas in the TI regime local pressure or velocity fluctuations caused by the small vortices lead to a deformation of the droplet. In high-pressure homogenizers, different flow conditions can prevail in different areas, which is why investigations are particularly difficult. Kolb et al. (2001) and Budde et al. (2002) have carried out the first optical investigations of drop break-up during high-pressure homogenization in scaled setups. These investigations were able to show that the drop break-up takes place in the area of the free jet behind the orifice. Due to the technical significance of the turbulent drop break-up, the number of investigations on this topic has increased significantly in recent decades. On the one hand, the number of experimental investigations examining the turbulent droplet break-up in test facilities using imaging techniques has increased e.g. Innings and Trägårdh (2005). On the other hand, the number of simulations on droplet break-up has increased e.g. Maniero et al. (2012). The aim of this project is to find out if the droplet break-up in high pressure homogenizers is driven by the droplet stretching in the laminar flow regime or the turbulent stresses acting on the droplets.

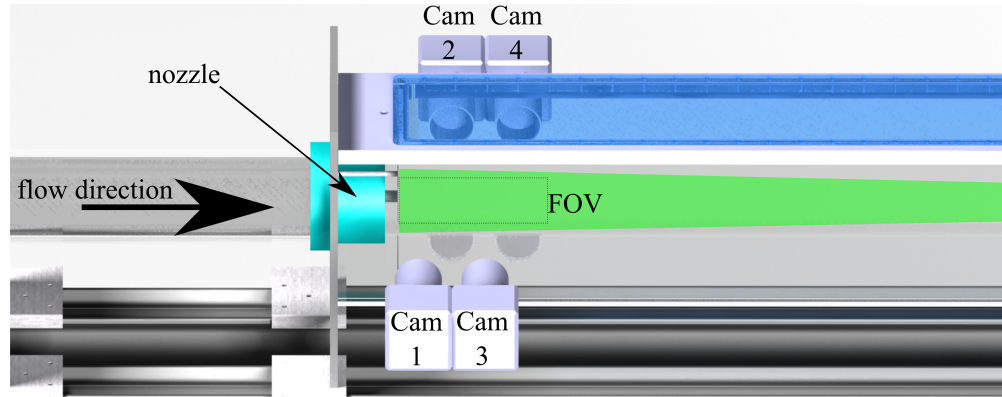


Figure 2: Camera and laser setup for the 2D2C-PIV measurements.

### 3 Setup

For the investigation of drop break-up during emulsification in high-pressure homogenizers, a scaled test plant was designed and constructed. Since image-based measuring methods are required to investigate the drop deformation and the drop break-up, the measuring section was made of glass and acrylic glass. The measuring section consists of an acrylic glass orifice plate with a constriction of the cross section from 100 mm inlet channel diameter (round) to an orifice diameter ( $d$ ) of 10 mm (round). The inlet edge of the constriction is rounded ( $R = 2d$ ). The length of the cylindrical orifice section is  $2d$ . Behind the orifice plate, the channel expands sharply to a rectangular channel with an edge length of 200 mm. Like the inflow area, this is made of glass. 2D2C PIV was used to characterize the mean flow properties in the test facility. Four PCO edge 5.5 sCMOS cameras with a resolution of  $2160 \times 2560$  px and a frame rate of 10 Hz were used simultaneously as illustrated in figure 2. A Quantel Evergreen 200 laser was used for the illumination of the tracer particles. The light sheet had a thickness of about 1 mm. The images were evaluated with the Davis 8.4 software from Lavisision by using an iterative multi-pass algorithm. The final interrogation window size was  $16 \times 16$  pixels with 50% overlap. After the evaluation, the recordings of the four cameras were combined with Matlab into a single data set.

To investigate the drop break-up during the emulsification of oil drops in an aqueous phase, oil drops could be introduced into the flow directly before the orifice plate through a flow-optimized inlet and a capillary. The droplets were generated outside of the test plant (see figure 1 top left). The droplets were visualized by means of shadowgraphy. In order to be able to observe the entire droplet break-up process in detail and along the FOV, several high-speed cameras were used for these measurements. The cameras were focused on the location of the drop break-up from two different directions. The angle between the cameras was  $90^\circ$ . This experimental setup made it possible to precisely determine the position in space behind the orifice and also to reconstruct and analyze the 3D shape of the droplets. Four Photron Fastcam SA-Z cameras at 40 kHz recording frequency were used for the measurements. The background illumination was provided by homogeneous LED panels (CCS TH2, Stemmer Imaging AG) with highly directional light. Figure 3 shows the camera setup for these measurements.

Preliminary investigations have shown that the basic shadowgraphy technique is not well suited for the visualization of oil droplets in the aqueous phase (see left image in figure 4), which is why a modification of the method was developed. The homogeneously illuminated background is broken up by a semi-transparent checkerboard pattern. This modification makes the light refraction at the interface clearly visible and the drop can be recognized with far more details. Figure 5 illustrates the basic and the modified shadowgraphy method.

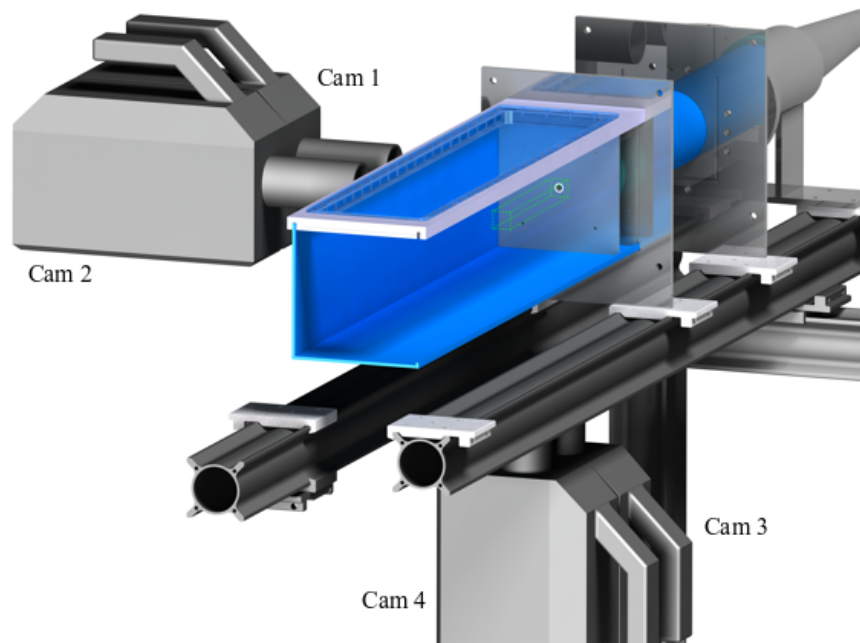


Figure 3: Camera setup for the high-speed shadowgraphy measurement of the oil drops.

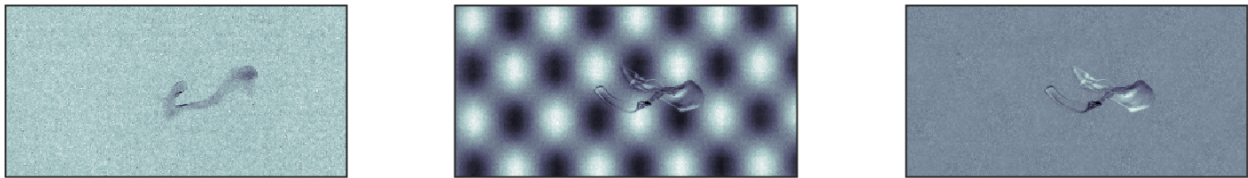


Figure 4: Comparison of drop visualization with normal shadowgraphy method (left), improved shadowgraphy method (center) and improved shadowgraphy method with background correction (right).

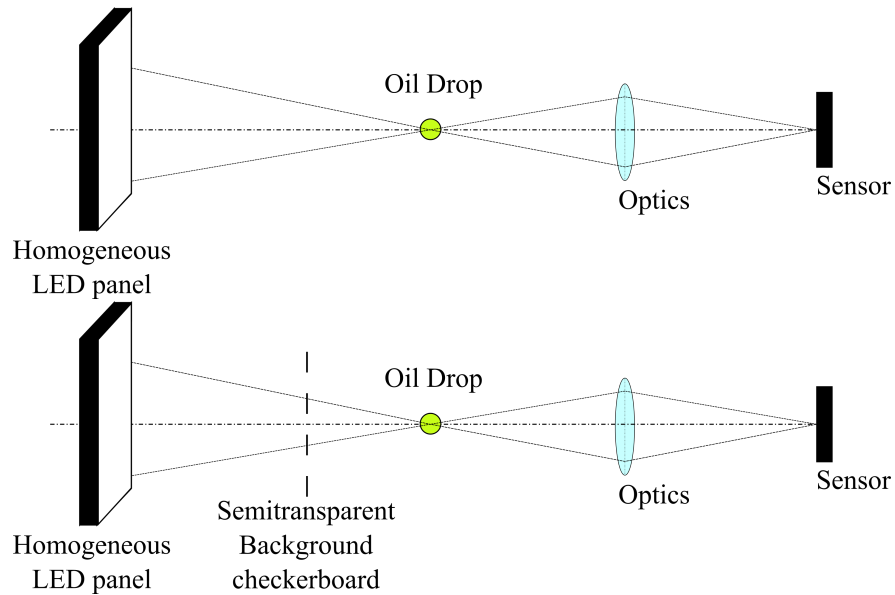


Figure 5: Schematic comparison of the normal shadowgraphy method (top) and the modified shadowgraphy method with background modulation (bottom).

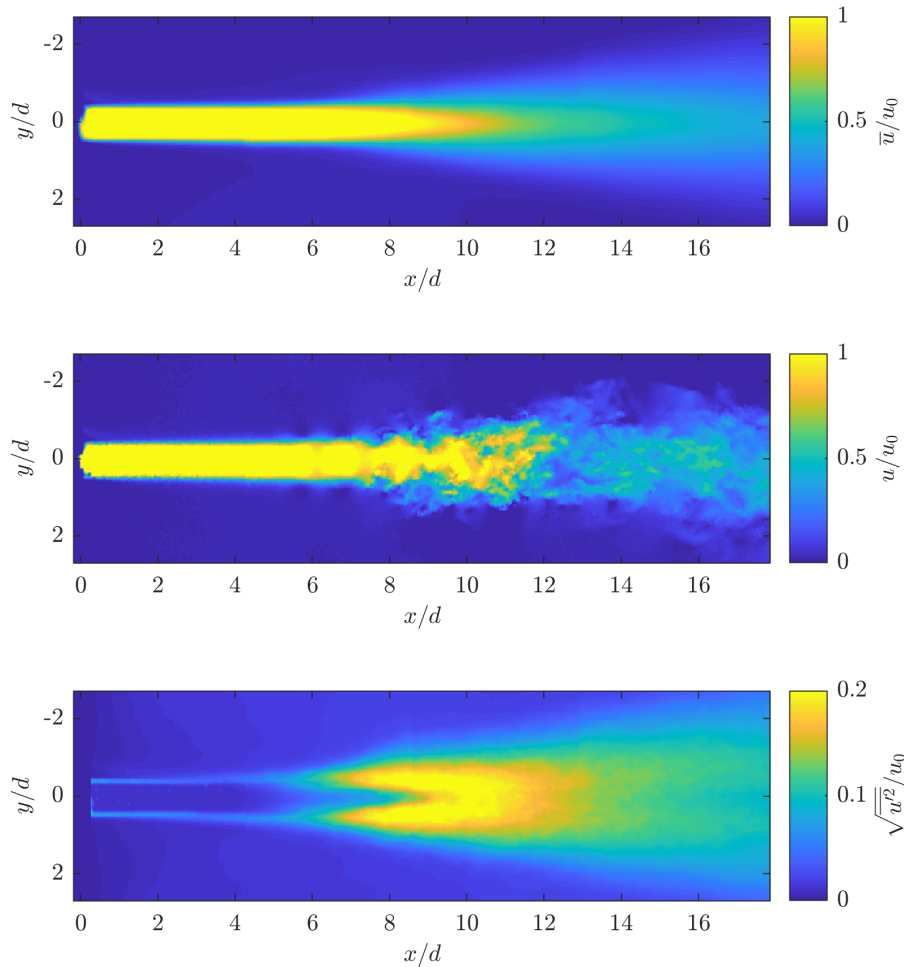


Figure 6: Flow profiles at  $Re = 2000$ : Top: time-averaged flow profile. Middle: instantaneous flow profile. Bottom: time-averaged velocity fluctuations in each case in flow direction  $x$  and normalized to the theoretical outlet velocity of the orifice plate.

## 4 Results

The single-phase flow characterization was performed at 2 Reynolds numbers in order to investigate different flow phenomena. The Reynolds numbers examined are  $Re = 2000$  and  $Re = 5700$ . Figure 6 shows 3 flow fields at the lower Reynolds number ( $Re = 2000$ ). The upper flow field shows the averaged flow field in  $x$  direction normalized to the average theoretical orifice exit velocity. The free jet is very symmetric on average and the core area extends approximately 8 orifice diameters downstream. The core of the free jet is surrounded by a shear layer which is very thin at the orifice outlet and expands inwards and outwards in the course of the free jet due to flow instabilities and turbulent mixing. As a result, the jet expands and the speed decreases. The flow field shown in the middle is an instantaneous flow field of the free jet also normalized with the theoretical orifice exit velocity. In this image, it becomes clear that the core of the free jet is also instantaneously stable up to approximately 6–7 orifice diameters. Thereafter oscillations start to occur and the jet decays after this running length. The image below shows the velocity fluctuations in flow direction normalized to the theoretical orifice exit velocity. In this illustration, the laminar core of the free jet is clearly visible, since there are hardly any velocity fluctuations in this region. The area is bordered by the shear layer in which the velocity fluctuations are significantly higher. They reach their maximum in the range of 8–11 orifice diameters downstream of the orifice.

The velocity fields in  $x$  direction of the higher Reynolds number  $Re = 5700$  are shown in figure 7.

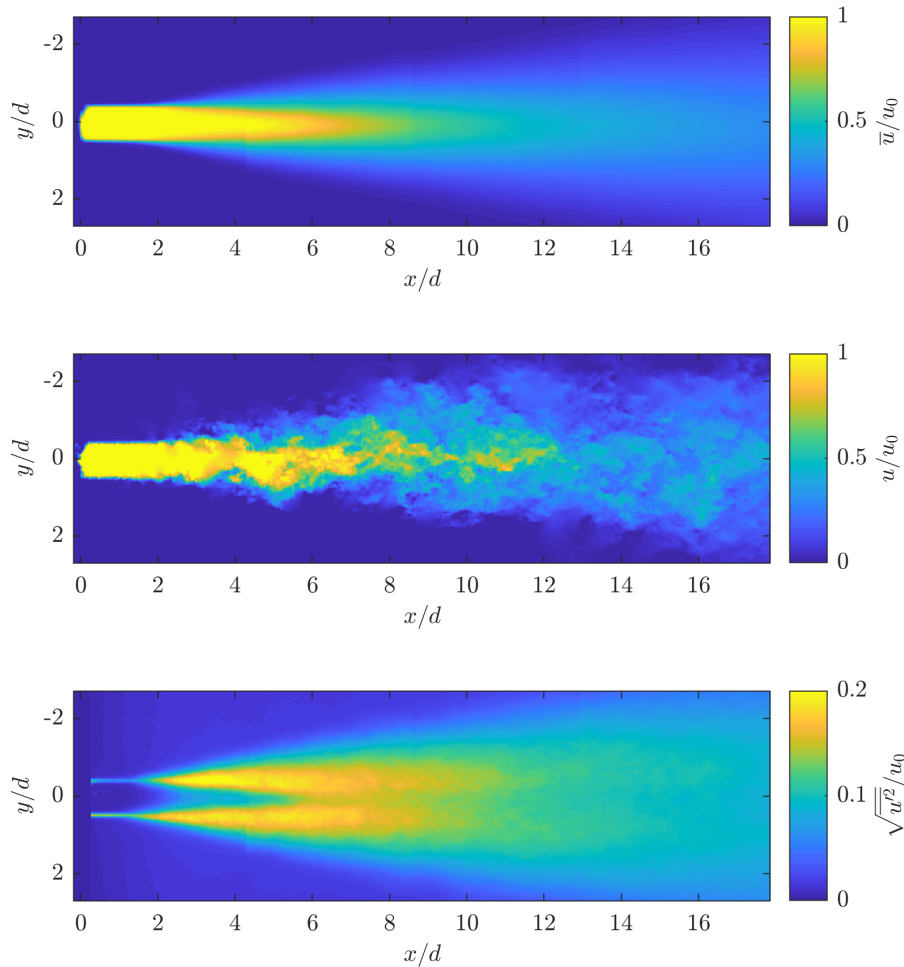


Figure 7: Flow profiles at  $Re = 5700$ : Top: time-averaged flow profile. Middle: instantaneous flow profile. Bottom: time-averaged velocity fluctuations in each case in flow direction  $x$  and normalized to the theoretical outlet velocity of the orifice plate.

The results are shown analogous to those in figure 6 normalized by the theoretical orifice exit velocity. In contrast to the results at  $Re = 2000$ , the stable free jet is significantly shorter. At approx. 2–4 orifice lengths, the free jet core begins to decay. As a result, the velocity fluctuation peaks are shifted forwards towards the orifice. In comparison to the theoretical orifice exit velocity, the velocity fluctuations are of the same relative intensity of approximately 20 %, but the absolute values are significantly higher as they scale with the Reynolds number.

For the drop break-up, it could be shown in previous investigations with the help of the 3D location determination that the break-up position lies within the area of the turbulent shear layer. The drop break-up is therefore significantly influenced by the instantaneous vortices and not by the average velocity variations. Therefore, the instantaneous velocity fields were analyzed in more detail to examine the connection between droplet break-up and turbulent vortices more thorough. The velocity field shown in Figure 8 shows the instantaneous velocity deviation from the mean value. In addition, the detected vortices are shown. The vortices were found using an algorithm based on the paper by Graftieux et al. (2001). It is evident that vortices develop towards the end of the free jet core in the shear layer. These vortices are caused by a Kelvin-Helmholtz instability and they become quite large and strong after a certain developing length. Further downstream the vortex size decreases due to turbulent mixing and diffusion, until in the rear part several small vortices unite to larger ones. The vortex strength, not shown here, decreases in the course of the free jet along with the vortex size due to friction and vortex splitting.

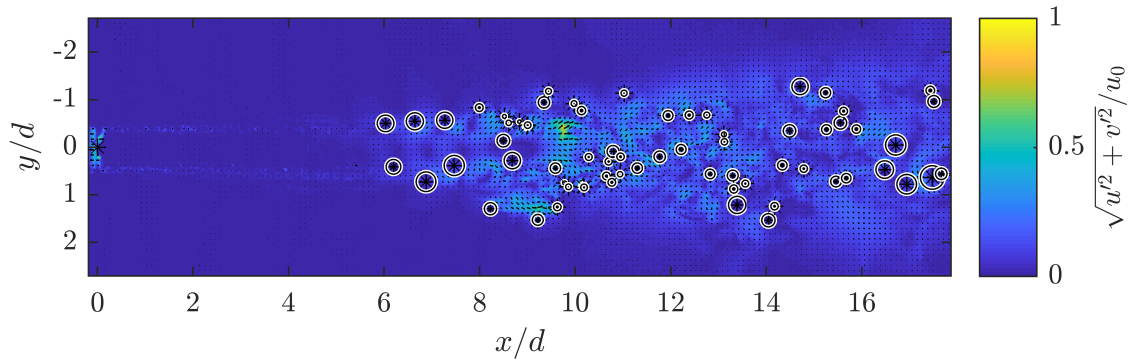


Figure 8: Instantaneous image of the detected vortex structure in the free jet behind the orifice. In the background the local instantaneous velocity fluctuation.

Based on these results the droplet break-up was investigated by shadowgraphy. The time series of shadow images of the oil drop passing through the orifice shown in Figure 9 illustrates the drop break-up at a Reynolds number of  $Re = 2000$ . The viscosity ratio of the investigated system is 3. The axes are normalized with the orifice diameter  $d$ . The origin lies on the symmetry axis of the orifice at the exit point of the free jet out of the orifice. At the beginning, in front of the orifice, the round output drop can be seen. The outlet droplet diameter is approx. 2–3 mm. When entering the orifice the round drop is deformed and elongated to a cylindrical drop. The aspect ratio of the droplet immediately after leaving the orifice is approx. 10–15. In the further course this droplet remains in the free jet core area, since the droplet feed has taken place on the symmetry axis. Due to the low stress in the core area, the droplet relaxes slightly, so that the aspect ratio decreases to approx. 8–10 at the end of the laminar core region of the jet. At the end of the core area at approximately 10 orifice diameters or after approximately 17.5 ms after leaving the orifice an obvious deformation of the drop is visible. The droplet is twisted in an S-shape due to the turbulent stresses acting on the drop. In the further course the droplet is interacting with several vortices. Thus it is twisted further, but also stretched and elongated. As a result of this stretching a very long twisted filament is formed which finally breaks up in an eruptive process. This indicates that some instability mechanism must finally be responsible for the breakup.

Lower viscosity drops or systems with a lower viscosity ratio are more strongly deformed or stretched in the laminar elongation flow of the orifice, while higher viscosity drops or systems with a higher viscosity ratio are less strongly stretched. Anyhow, the break-up behind the orifice is happening in a similar manner by capturing the drop by vortices and breaking it up. The vortices initially always stretch the droplet and ultimately tear the filament apart. Depending on the origin of the droplet in the free jet, the droplet deformation can begin with the droplet slowly swinging up when large vortices initially cause a slight deformation. Due to the oscillation and meandering of the droplet, the droplet finally enters the shear layer, where velocity gradients or small vortices lead to strong small-scale deformations and the associated extreme elongation of the droplet. As a result of this strong elongation, the droplet finally breaks up.

In addition to the viscosity ratio, the droplet break-up is determined to a large extent by the point at which the droplets pass through the orifice. This parameter is relevant because the droplet is therefore more likely to enter the turbulent shear layer of the free jet at an early point in space. In order to investigate this relationship more closely, the droplet was placed at various positions in front of the orifice plate by using a special designed feeding device. The dimensionless radius  $r^*$  was selected to characterize the droplet feed position. This describes the droplet feed position as the distance to the axis of symmetry relative to the maximum possible radius of the flow channel in front of the orifice plate. Figure 10 shows three different images of the break-up of droplets feed into the channel from three different radial positions. The image shown was selected for each case individually, as the drop break-up is most clearly visible. What is noticeable when comparing the three cases shown in Figure 10 is that the point of break-up moves closer to the orifice plate when the  $r^*$  is increased. It also becomes clear that drop break-up does not take place as a simultaneous event over the entire drop length, but takes place in individual areas independently of each other. These areas are characterized by locally increased turbulence or the presence of small intense vortices. These lead to a locally strongly pronounced deformation of the droplet, which ultimately leads to the break-up of the droplet. The results show clearly the strong relation between turbulence and droplet break-up. Furthermore the analysis illustrates that the laminar droplet break-up due to the Plateau–Rayleigh

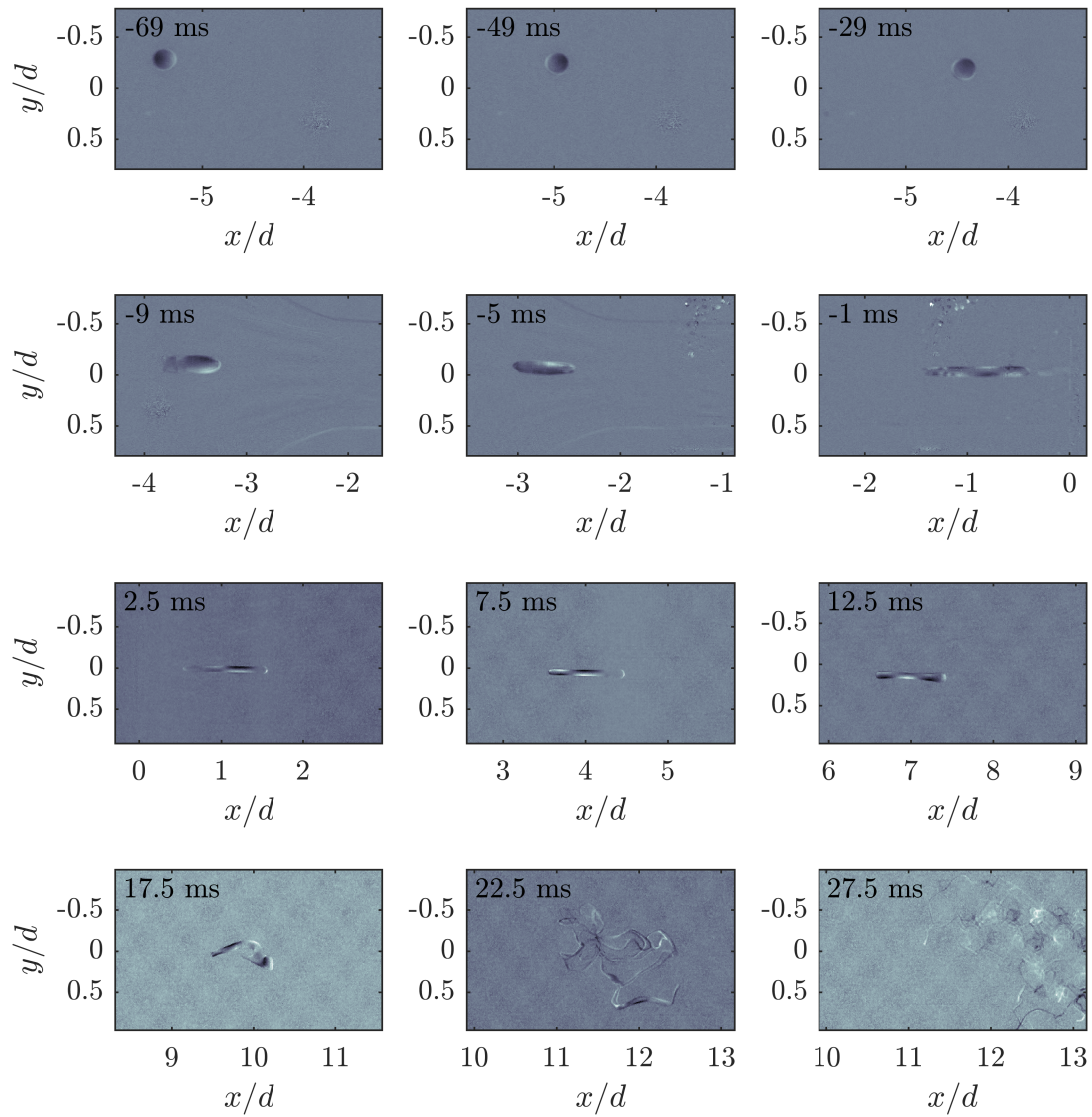


Figure 9: Visualisation of the spatial and temporal course of the drop through the orifice and the break-up behind the orifice in the turbulent shear layer.

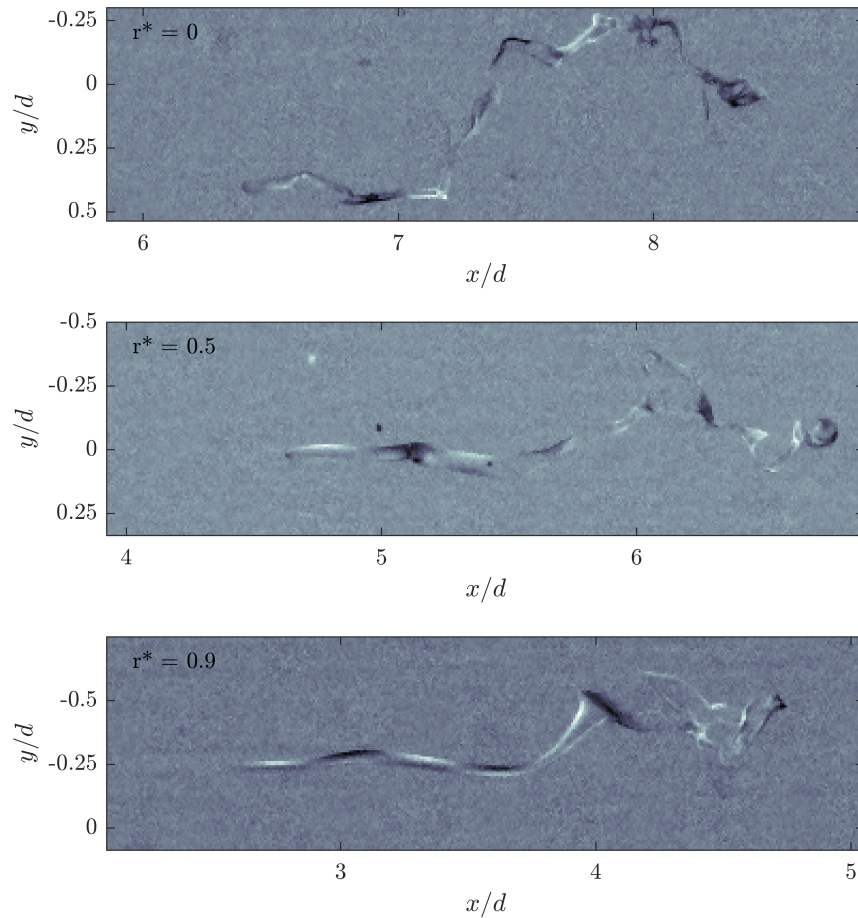


Figure 10: Comparison of the break-up scheme of the oil drop behind the orifice plate in the shear layer at different dosing positions  $r^*$  (top:  $r^* = 0$ ; middle:  $r^* = 0.5$ ; bottom:  $r^* = 0.9$ ).

instability plays no significant role at large Reynolds numbers.

## 5 Conclusion

The investigation shows that the scaled flow experiment is well suited to examine the stretching, deformation and break-up of a droplet due to the convective acceleration and turbulent action. These investigations show that the droplet break-up at high Reynolds numbers is mainly caused by turbulence, i.e. by the vortex size and strength. It also becomes clear from the investigations that the drop break-up is not happening at a uniform stream-wise location, since drops can have different trajectories in front of, inside and especially behind the orifice plate. In particular, the stochastic behavior of the free jet's turbulence behind the orifice plate leads to different stress profiles for otherwise identical drops and identical drop feed positions. These differences, which even with a single droplet result in different response characteristics, mean that the droplet size distribution generated during high-pressure homogenization is not mono disperse, but rather produces a wide size distribution. To enhance the turbulence in the shear layer for more efficient droplet break-up nozzles with vortex generators may be advantageous.

## Acknowledgements

The authors thank the German Research Foundation (DFG) for the financial support of the project "Investigations on the measurement of the relevant flow conditions for the deformation and break-up of droplets during high-pressure homogenization with orifices and on the scalability of the methods" (KA 1808/19-1). Discussions with Peter Walzel (TU Dortmund) about scaling properties of the facility and liquid properties are greatly appreciated.

## References

- Budde C, Schaffner D, and Walzel P (2002) Modellversuche zum Tropfenzerfall an Blenden in Flüssig/Flüssig/Dispersionen. *Chemie Ingenieur Technik* 74:101–104
- Graftieaux L, Michard M, and Grosjean N (2001) Combining PIV, POD and vortex identification algorithms for the study of unsteady turbulent swirling flows. *Measurement Science and Technology* 12:1422–1429
- Innings F and Trägårdh C (2005) Visualization of the drop deformation and break-up process in a high pressure homogenizer. *Chemical Engineering & Technology* 28:882–891
- Kähler CJ, Astarita T, Vlachos PP, Sakakibara J, Hain R, Discetti S, La Foy R, and Cierpka C (2016) Main results of the 4th international piv challenge. *Experiments in Fluids* 57:97
- Kolb G, Wagner G, and Ulrich J (2001) Untersuchungen zum Aufbruch von Einzeltropfen in Dispergiereinheiten zur Emulsionsherstellung. *Chemie Ingenieur Technik* 73:80–83
- Maniero R, Masbernat O, Climent E, and Risso F (2012) Modeling and simulation of inertial drop break-up in a turbulent pipe flow downstream of a restriction. *International Journal of Multiphase Flow* 42:1 – 8
- Mighri F and Huneault MA (2006) In situ visualization of drop deformation, erosion, and breakup in high viscosity ratio polymeric systems under high shearing stress conditions. *Journal of Applied Polymer Science* 100:2582–2591
- Mutsch B and Kähler CJ (2017) Charakterisierung eines Versuchsstands zur Messung der relevanten Strömungsbedingungen für die Deformation und den Aufbruch von Tropfen beim Hochdruckhomogenisieren mit Blenden. *Experimentelle Strömungsmechanik* 25
- Taylor GI (1934) The formation of emulsions in definable fields of flow. *Proceedings of the Royal Society of London Series A, Containing Papers of a Mathematical and Physical Character* 146:501–523
- Walstra P (1993) Principles of emulsion formation. *Chemical Engineering Science* 48:333 – 349
- Walzel P (2015) personal communication